FTIR, XRF and Powder XRD Experimental Study of Charoite: Crystal Chemical Features of Two Associated Generations

Chapter · August 2020

DOI: 10.1007/978-3-030-49468-1_13

CITATIONS
0

READS
13

6 authors, including:

Ekaterina Kaneva
Vinogradov Institute of Geochemistry SB RAS
59 PUBLICATIONS **52** CITATIONS

SEE PROFILE

Tatiana Alexandrovna Radomskaya
Vinogradov Institute of Geochemistry SB RAS
8 PUBLICATIONS **8** CITATIONS

SEE PROFILE

Roman Shendrik
Vinogradov Institute of Geochemistry SB RAS
91 PUBLICATIONS **215** CITATIONS

SEE PROFILE

FTIR, XRF and Powder XRD Experimental Study of Charoite: Crystal Chemical Features of Two Associated Generations

Ekaterina V. Kaneva, Tatiana A. Radomskaya, Roman Yu. Shendrik, Victor M. Chubarov, Alena A. Amosova, and Mikhail A. Mitichkin

Abstract

A collection sample of charoite rock from the Murun massif (Russia) was examined. Based on the textural and structural features, it was concluded that the sample comprised two charoite generations: the earliest one, so-called "block", and the second one, "schistose-goffered". A small amount (1–2 g) of each phase was used for sequential X-ray diffraction, X-ray fluorescence and FTIR absorption analyses. The obtained results allowed us to reveal some crystal chemical features of the early and later generations of the charoite specimen under study.

Keywords

Charoite · The Murun massif · Crystal chemistry · FTIR

1 Introduction

Charoite, $(K,Sr,Ba,Mn)_{15\text{-}16}(Ca,Na)_{32}[Si_{70}(O,OH_{180}](OH,F)_4 \cdot nH_2O$, is a unique valuable jewelry-ornamental stone, found only in alkaline rocks of the Murun massif (Yakutia, Russia). The mineral was originally described in 1978 (Rogova et al. 1978), and the crystal structure of charoite was solved only in 2009 using the

E. V. Kaneva (✉) · T. A. Radomskaya · R. Yu. Shendrik · V. M. Chubarov · A. A. Amosova · M. A. Mitichkin
Vinogradov Institute of Geochemistry SB RAS, 1A Favorsky str., 664033 Irkutsk, Russia
e-mail: kev604@mail.ru

E. V. Kaneva · T. A. Radomskaya · V. M. Chubarov
Irkutsk National Research Technical University, 83 Lermontov str., 664074 Irkutsk, Russia

S. Votyakov et al. (eds.), *Minerals: Structure, Properties, Methods of Investigation*,
Springer Proceedings in Earth and Environmental Sciences,
https://doi.org/10.1007/978-3-030-49468-1_13

methods of automatic electron diffraction tomography (ADT) and precession electron diffraction (PED) (Rozhdestvenskaya et al. 2010). Two polytypes with different unit cell parameters were identified: monoclinic "charoite-96" (Rozhdestvenskaya et al. 2010) and monoclinic, but with a pseudorhombic cell, "charoite-90" (Rozhdestvenskaya et al. 2011). In addition, there are other partially ordered and disordered polytypes ("charoite-2a" and "charoite-d" (Rozhdestvenskaya et al. 2011)), which are extremely rare. The crystal structure of charoite contains three different types of silicon-oxygen chains attached to a ribbon of Ca- and Na-octahedra extending along the [001] direction. The cavities formed in the structure are occupied by (K,Sr,Ba,Mn)-cations and H_2O molecules.

2 Materials and Methods

The sample under study is a piece of charoite rock that was polished on one side, 6.5 × 4.0 × 1.0 cm in size. It is composed of two generations of charoite (Fig. 1). The first, earliest generation (~75 vol.% of the sample) is the so-called "block" charoite (according to Vorob'ev (2008)). The aggregate is composed of densely accreted and elongated in one direction parallel-columnar thinnest charoite fibers. The length of individual crystals reaches 3–4 cm with a width of 1–2 μm. When exposed to light at different angles, the "block" charoite changes its color from light lilac with a characteristic silky shine to dark purple. There are four areas in the sample (1a, 1b, 1c and 1d on Fig. 1), inside which the charoite fibers are oriented equally relative to each other, but at an angle relative to the charoite fibers in the adjacent area. The width of the area varies from 0.5 to 2.0 cm.

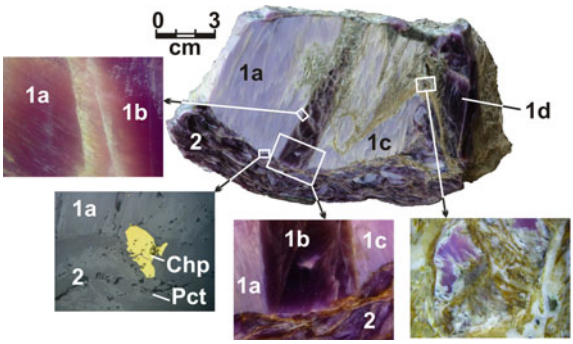

Fig. 1 The polished side of the sample with two generations of charoite: 1a, 1b, 1c, 1d—early "block" generation with different orientation of charoite crystal fibers in different blocks; 2—"schistose-goffered" generation of charoite. Cha—charoite, Chp—chalcopyrite

The second generation of charoite occupies about 15 vol% of the sample. It is assigned to the "schistose-goffered" morphological modification (according to Vorob'ev (2008)). The needle-fibrous crystals of charoite grow together tightly into numerous small aggregates, up to 0.5–1.0 cm long and up to 0.2 mm wide, which gives a slate-curved texture of this generation (2 on Fig. 1). The color of the "schistose-goffered" aggregates changes from light purple with a silky shine to dark violet. The small grains of pectolite in small quantities are associated with this charoite.

Copper and lead sulfides were found among charoite aggregates. Moreover, the intergrowth of galena and chalcopyrite was detected in the early generation ("block" charoite) (Fig. 1), whereas in the late generation ("schistose-goffered") charoite, chalcopyrite grains were found, sometimes in paragenesis with sphalerite. A part of the chalcopyrite grains was located on the border of various generations of charoite. The unpolished side of the sample was affected by secondary changes: here charoite was replaced by apophyllite. On the polished side of the sample, apophyllite filled the cracks.

Due to the fact that the sample has a decorative, artistic and commercial value, it cannot be destroyed. Therefore, a realization of analytical routines for the sample investigation was a difficult task. For the study of both generations, the minimum required amount of material was selected ($\sim$1–2 g). The samples were sequentially used for all types of analyses mentioned below.

The chemical composition was determined by the X-ray fluorescence method. Measurements were performed by a S4 Pioneer wavelength-dispersive X-ray fluorescence spectrometer (Bruker AXS, Germany). The powders were calcinated at 950 °C to determine the loss on ignition (LOI) values. Then a portion (500 mg) of calcinated sample was mixed with 7.5 g of lithium borate flux (33% of lithium metaborate and 67% of lithium tetraborate) with the addition of 7 drops of 4% LiBr solution) and fused in platinum crucibles in a TheOX (Claisse, Canada) electric furnace at 1050 °C. The calibration equation was constructed using the certified reference materials of igneous and sedimentary rocks.

Powder X-ray diffraction data were obtained using a D8 ADVANCE diffractometer (Bruker) equipped with a scintillation detector and a Göbel mirror. The radiation source was CuKα. The data were recorded in the step-scan mode in the range of 2θ diffraction angles from 3 to 80°. Experimental conditions were the following: 40 kV, 40 mA, time per step—1 s and step size—0.02° 2θ. The data processing was performed using the DIFFRACplus software package. The unit cell parameters were refined using TOPAS 4 software (Bruker 2008).

Infrared absorption spectra were obtained using an FT-801 FTIR spectrometer (Simex). Charoite was mixed with pre-dehydrated KBr and compressed into a tablet weighing 20 mg. The infrared spectra were acquired from 5300 to 450 cm^{-1}.

3 Results and Discussion

The results of the wavelength-dispersive X-ray fluorescence analysis of powder samples of two charoite generations under study are given in Table 1. The sum of the components is somewhat underestimated as compared, for example, with the data by Gladkochub (2016) (~93 wt% *vs* 95–96 wt%). However, they are consistent with the data by Rozhdestvenskaya (2010) (~93 wt% *vs* 92 wt%). Losses on ignition (LOI) are 6.51 and 6.55% for generations 1 and 2, respectively. In our samples, the Na_2O and K_2O content is lower relative to Rozhdestvenskaya et al. (2010) and Gladkochub (2016) (possibly included in the LOI).

Table 1 also presents the calculated parameters of the unit cell of the two polytype using the TOPAS software (Bruker 2008). The initial unit cell parameters and the atomic coordinates required for the calculations were taken from Rozhdestvenskaya et al. (2010) for "charoite-90" and Rozhdestvenskaya et al. (2011) for "charoite-96", respectively. According to Rozhdestvenskaya and Drits (2013), monophasic specimens of charoite are extremely rare. In addition to the two polytypes, after careful selection, impurity phases remain in the samples, complicating the powder diffraction pattern. Thus, apophyllite and pectolite have been diagnosed in the samples.

The normalized infrared absorption spectra of two charoite generations are given in Figs. 2 and 3. The group of peaks at 1116, 1100, 1084, 1056, 1015, 958, 935 cm^{-1} (Fig. 2) are assigned to asymmetric Si-O stretching modes of the SiO_4 tetrahedra, while the sharp peak in mid-frequency range from 703 to 610 cm^{-1} can

Table 1 Experimental crystal chemical data for the "block" and "schistose-goffered" generations of charoite, obtained by X-ray fluorescence and X-ray diffraction analyses

"Block generation" (1a, 1b, 1c and 1d on Fig. 1)				"Schistose-goffered generation" (2 on Fig. 1)			
Chemical composition according to XRF data (wt%)							
SiO_2	59.21	Al_2O_3	0.21	SiO_2	58.68	Al_2O_3	0.11
Na_2O	1.98	K_2O	7.51	Na_2O	1.80	K_2O	7.66
CaO	21.08	MnO	0.19	CaO	21.61	MnO	0.20
BaO	2.03	Sr	0.81	BaO	1.96	Sr	0.79
Zr	0.01	LOI	6.51	Zr	0.01	LOI	6.55
Total	99.54			Total	99.37		
Unit cell parameters for the polytypes (Å, °, $Å^3$), sp. gr. $P2_1/m$							
"charoite-90"							
a = 32.05(1); b = 19.67(1); c = 7.16(1); β = 90.07(2); V = 4514(2)				a = 32.08(2); b = 19.68(1); c = 7.16(1); β = 90.03(7); V = 4523(4)			
"charoite-96"							
a = 32.20(2); b = 19.67(1); c = 7.24(1); β = 94.87(4); V = 4570(3)				a = 32.19(3); b = 19.67(2); c = 7.25(1); β = 94.97(5); V = 4570(6)			
Ratio "charoite-90":"charoite-96" (%)							
75:25				70:30			

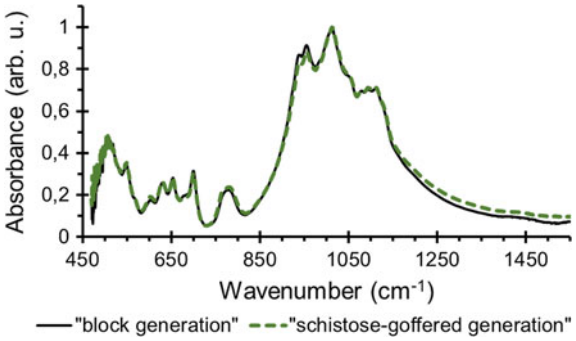

Fig. 2 Relative absorbance of the "block" and "schistose-goffered" generations of the studied charoite (450–1550 cm^{-1} range of absorption spectra)

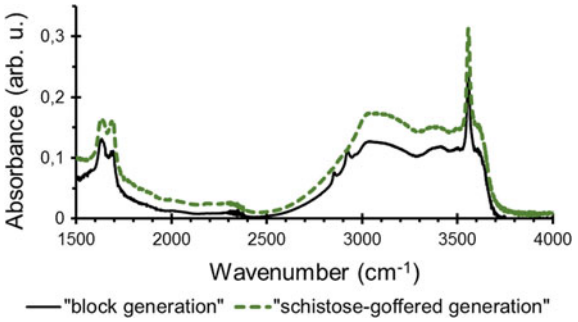

Fig. 3 Relative absorbance of "block" and "schistose-goffered" generations of the studied charoite in the water absorption region of spectra

be attributed to Si-O-Si bending mode as well as symmetric O-Si-O stretching vibrations (Infrared et al. 2001). Peaks at about 570 and 787 cm^{-1} can be assigned to symmetric Si-O and O-SiO vibrations, respectively (Gittins et al. 1976). The peak at about 553 cm^{-1} can correspond to the Ca-O stretching.

The band positions observed in the 1500–1400 cm^{-1} range and their assignment are given in Table 2. The table also contains the literature IR data for charoite. In charoite samples, strong wide bands in the 3000–3700 cm^{-1} spectral region correspond to symmetric and asymmetric stretching vibration of H_2O molecules (Fig. 3); they are bands peaked at 3111, 3429 and 3597 cm^{-1}. The sharp peak at 3556 cm^{-1} can correspond to stretching modes of OH-ions. Two bands in the region of 1631 and 1688 cm^{-1} are associated with the H_2O bending vibrations. Both samples contain similar amounts of SiO_2 and CaO. Therefore, a comparison of H_2O and OH amounts in the samples can be related to the OH and H_2O band

Table 2 Band position (cm^{-1}) of H_2O and OH in the IR spectra of the studied charoite samples and literature data

This study	Lacalamita (2018)	Rogova (1978)	Band assignment
1688, 1631	1667, 1595	1650, 1620, 1590	H_2O bending
3111, 3429, 3597	3453, 3385, 3285, 3150	3610, 3550, 3500, 3410	H_2O stretching
3556	3530		OH stretching

intensities with symmetric Si-O or Ca-O stretching modes. In general, the position and configuration of the bands in the frequency range of the H_2O and OH vibrations of both samples show a complete analogy, but there are slight differences in their intensities. The result indicates an increased content of H_2O and OH groups in the charoite sample, which belongs to the second, "schistose-goffered generation".

Figure 4 shows the thermal dehydroxylation curves of "schistose-goffered" generation of the charoite sample. There are bands measured at 3111, 3429, 3556, 3597, 1688 and 1631 cm^{-1} (Table 2). The figure shows the relative intensities of the hydroxyl and H_2O bands in the samples quenched over the temperature range from 25 to 750 °C at 50 °C intervals. The diagram clearly shows that there are three groups of lines. OH^- absorption (the band at 3556 cm^{-1}) disappears completely at 400 °C. For the bands at 3111 and 1688 cm^{-1}, assigned to the stretching and bending vibrations of H_2O, respectively, dehydroxylation mostly takes place at the 200 to 450–500 °C temperature range. The absorbance of another group of bands belonging to H_2O molecule vibrations (3429 cm^{-1}—stretching and 1631 cm^{-1}—bending) drops to zero at 650 °C. Finally, for the band at 3597 cm^{-1}, dehydroxylation completely disappears above 750 °C.

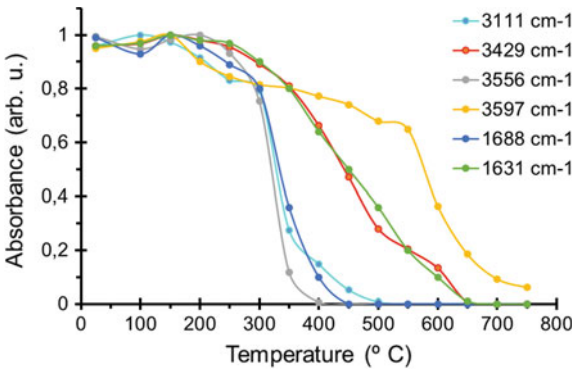

Fig. 4 Thermal dehydroxylation curves measured at 3111, 3429, 3556, 3597, 1688 and 1631 cm^{-1} for the "schistose-goffered generation" of the studied charoite sample

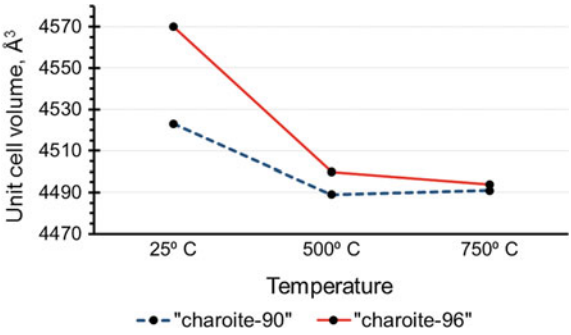

Fig. 5 The dependence of the change in the unit cell volume on temperature for "charoite-90" and "charoite-96" polytypes of the "schistose-goffered generation"

Thus, there are three water environments in the charoite structure with different removal temperatures. This fact confirms the results of the "charoite-90":"charoite-96" ratio calculation (Table 1) and verifies the prevalence of the "charoite-90" polytype in the sample. It contains three H_2O sites (Rozhdestvenskaya et al. 2010), while the "charoite-96" has only one H_2O site in the crystal structure model (Rozhdestvenskaya et al. 2011).

Investigating the process of dehydroxylation of the generation more enriched in water, it is necessary to pay attention to the changes in the unit cell parameters. Using the TOPAS software (Bruker 2008), the unit cell volumes of "charoite-90" and "charoite-96" polytypes in the "schistose-goffered" sample were calculated after heating at 500 and 750 °C. The dependence of the volume of the unit cell on temperature is shown in Fig. 5. It is clearly visible that the unit cell volume significantly decreases at 500 °C, corresponding to the H_2O and OH-group removal from the structure. Then, when heated to 750 °C, the unit cell volume ceases to change greatly. However, according to IR spectroscopy and XRD data, the second type of H_2O is removed from the crystal structure without any obvious effect on its unit cell parameters in the range from 500 to 750 °C (at about 650 °C, see Fig. 4).

The "charoite-90":"charoite-96" ratio does not change after heating. It means that one modification of charoite does not transfer into another.

4 Conclusions

According to the textural and structural features of the sample under study, two generations of charoite have been distinguished. They are similar in chemical composition and crystal structural features. However, as it follows from the obtained data, the processes of formation of the early generation ("block") occurred with a low rate of change in the temperature gradient. It led to the crystallization of

long parallel-columnar fibers forming block aggregates of charoite. The residual mineral-forming media seems to contain a greater amount of aqueous fluid and impurities. It led to the crystallization of the late generation "schistose-goffered" charoite.

Acknowledgements The study was performed using the equipment of the "Isotopic-geochemistry investigations centre" of Collective Use Center of A.P. Vinogradov Institute of Geochemistry SB RAS.
This work was supported by the grant of the President of the Russian Federation No. MK-936.2019.5.
The experiments on thermal dehydroxylation were supported by the grant of the Russian Science Foundation RSF 18-72-10085.

References

Bruker AXS. Topas V4: General profile and structure analysis software for powder diffraction data (User's Manual, Bruker AXS, Karlsruhe, Germany). 2008.

Gittins J, Bown MG, Sturman D. Agrellite, a new rock-forming mineral in regionally metamorphosed agpaitic alkali rocks. Can. Min. 1976; 14:120–126.

Lacalamita M. Micro-FTIR and EPMA characterisation of charoite from Murun massif (Russia). J. Spectroscopy. 2018. https://doi.org/10.1155/2018/9293637.

Marchuk MV, Medvedev VYa, Ivanova LA, Sokolova TS, Danilov BS, Gladkochub DP. Charoite. Experimental studies. Geodyn. Tectonoph. 2016;7(1):105–118. https://doi.org/10.5800/GT-2016-7-1-0199.

Rozhdestvenskaya IV, Drits VA. Peculiarities of the charoite X-ray powder diffraction pattern. Zap. Vseross. Mineral. Obsh. 2013;142(4):101–112.

Rozhdestvenskaya I, Mugnaioli E, Czank M, Depmeier W, Kolb U, Merlino S. Essential features of the polytypic charoite-96 structure compared to charoite-90. Min. Mag. 2011;75(6):2833–2846. https://doi.org/10.1180/minmag.2011.075.6.2833.

Rogova VP, Rogov YG, Drits VA, Kuznetsova NN. Charoite, a new mineral, and a new jewelry stone. Zap. Vses. Mineral. Obsh. 1978;107(1):94–100. (In Russ.).

Rozhdestvenskaya I, Mugnaioli E, Czank M, Depmeier W, Kolb U, Reinholdt A, Weirich T. The structure of charoite, $(K,Sr,Ba,Mn)_{15\text{-}16}(Ca,Na)_{32}[Si_{70}(O,OH_{180}](OH,F)_4{\cdot}nH_2O$, solved by conventional and automated electron diffraction. Min. Mag. 2010;74(1):159–177. https://doi.org/10.1180/minmag.2010.074.1.159.

Socrates G. Infrared and Raman characteristic group frequencies: tables and charts. John Wiley & Sons Ltd., 2001.

Vorob'ev EI. Charoite. Academy Publishing "Geo", Novosibirsk, 2008. (In Russ.).